Metal-Free Catalysis

DOI: 10.1002/anie.200901826

Heteroatoms Increase the Selectivity in Oxidative Dehydrogenation Reactions on Nanocarbons**

*Benjamin Frank, Jian Zhang, Raoul Blume, Robert Schlögl, and Dang Sheng Su**

The surface of carbon materials is usually terminated by a variety of oxygen functional groups.[1,2] This chemical abundance has claimed an important role in many research areas.[3] Of these surface species, the ketonic and quinoidic groups are rich in electrons and thus have great potential to coordinate a redox process (Scheme 1). Lewis basic sites can abstract hydrogen atoms from C–H bonds of alkanes to produce the corresponding alkenes. The reaction of gas-phase oxygen with the abstracted hydrogen will regenerate the active sites, with formation of water as the product.[4,5]

One of the hottest topics in carbon chemistry is the use of nanostructured carbons, and especially carbon nanotubes (CNTs), as metal-free catalysts. Recent reports have shown an outstanding performance of nanoscaled carbon materials in the oxidative dehydrogenation (ODH) of hydrocarbons.[4,6] This progress opens new horizons for CNTs application and provides enormous possibilities to investigate the nature of ODH reactions on a fundamental level. In contrast to supported transition metal oxides, nanocarbon as a simple platform is highly adaptable to kinetic and mechanistic investigations of complex redox reactions. Our recent work has indicated a similar mechanism to that on vanadium oxide catalysts.[4,7] Furthermore, carbonaceous species can form on the surface of metal oxide catalysts during the ODH of propane,[8] which raises questions on the catalytic role of deposited carbon. In carbon-catalyzed ODH reactions, ethylbenzene is predominantly used as the substrate, as the stable conjugated system of the product styrene allows for high yields. In contrast, light alkanes are much less reactive than the corresponding alkenes.[9] Both the inferior selectivity and the yield of alkenes have so far retarded the industrial application of the ODH technology despite outstanding advantages of the oxidative pathway as compared to non-oxidative processes for alkene production.[10]

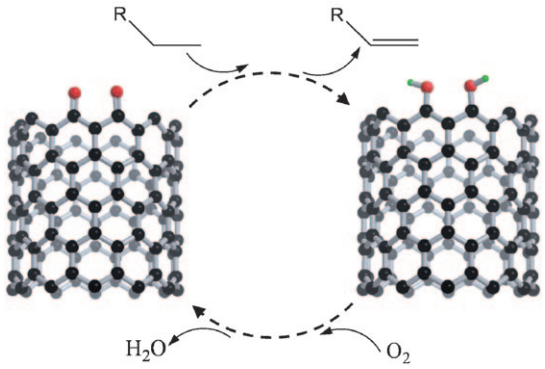

Scheme 1. The oxidative dehydrogenation of alkanes over functionalized CNTs.

Nucleophilic oxygen species, such as O^{2-}, inside the active domains have been identified as being the prerequisite for a high alkene selectivity. Unfortunately, the most likely intermediates during the activation of O_2 molecules, O_2^{2-}, O_2^-, and O^- are electrophilic and thus ultimately cause total oxidation, especially of the produced alkene, which has an electron-rich π bond.[11] The implementation of an electron-attracting dopant, such as boron or boron oxide, will reduce the generation of highly reactive oxygen species[12] and is thus expected to increase the selectivity to propene. Herein we report that boron-modified CNT catalysts are remarkably selective towards propene formation in the ODH of propane. Oxygen isotope exchange and transient experiments show that the activation of oxygen is optimized to yield a comparable selectivity with that of low-loaded vanadia catalysts. We demonstrate a sustainable metal-free strategy for propene synthesis that is free of the environmental burden of toxic transition metals.

For a comparative study of the catalytic performance in the ODH of propane, we evaluated pristine CNTs (CNTs), oxidized CNTs (oCNTs), and boron oxide modified CNTs (denoted as *x*B-oCNTs, with $x = 0.003$–5 wt% B_2O_3). A 5 wt% P_2O_5-loaded sample (5P-oCNTs) was prepared analogously.[4] The only products that were detected were propene, CO, CO_2, and H_2O. Reactions in the gas phase could be excluded by blank experiments. All the samples showed stable catalytic performance after a few hours time-on-stream and were investigated in detail by variation of flow rate and reaction temperature, periodic feed of oxygen and propane, and a test for dynamic oxygen exchange. As can be seen in Figure 1a, samples with boron oxide and phosphorus oxide have a superior selectivity towards propene formation than pristine CNTs and oCNTs. Such a pronounced enhancement can be related to the improved chemical stability after modification. Temperature-programmed oxidation (TPO) profiles reveal an increasing resistance to oxidation in the

[*] Dr. B. Frank, Dr. J. Zhang, Dr. R. Blume, Prof. Dr. R. Schlögl, Dr. D. S. Su
Department of Inorganic Chemistry
Fritz Haber Institute of the Max Planck Society
Faradayweg 4–6, 14195 Berlin (Germany)
Fax: (+49) 30-8413-4401
E-mail: dangsheng@fhi-berlin.mpg.de

[**] This work is financially supported by the EnerChem project (Max Planck Society). The authors gratefully acknowledge Prof. R. Schomäcker (Technische Universität Berlin), E. Kitzelmann, G. Weinberg, Dr. D. Rosenthal, and Dr. Bo Zhu for experimental assistance and fruitful discussions.

Supporting information for this article is available on the WWW under http://dx.doi.org/10.1002/anie.200901826.

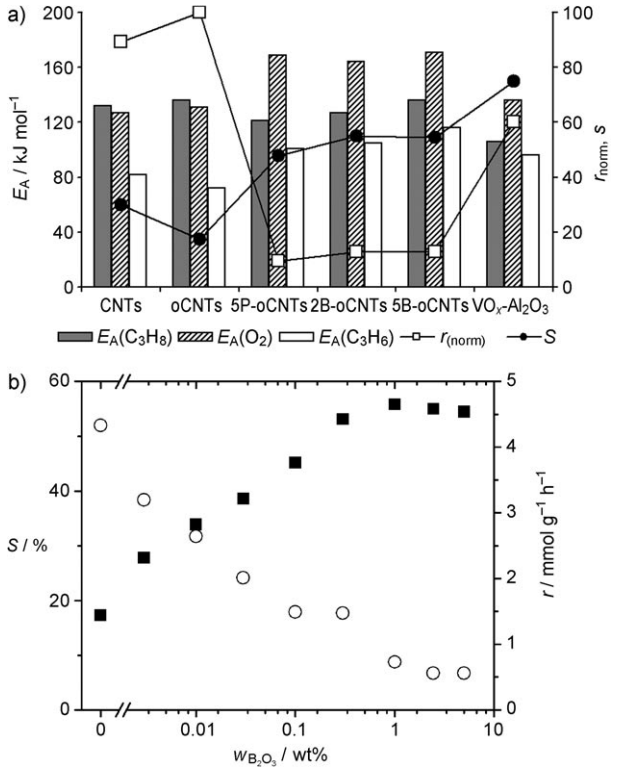

Figure 1. Catalytic performance of CNT catalysts in the ODH of propane, with VO_x-Al_2O_3 as a reference.[14] a) Apparent activation energies E_A of propane conversion, oxygen conversion, and propene formation (bars), and normalized activity r_{norm} and propene selectivity S (in %) at 5% propane conversion (symbols); b) propene selectivity at 5% propane conversion (■) and reaction rate r (○) as a function of B_2O_3 loading $w_{B_2O_3}$. Reaction conditions for CNT catalysts: 1 g, C_3H_8/O_2/N_2 = 1:1:4, 10–140 mL_n min^{-1}, 673 K.

order CNTs < oCNTs ≪ 2B-oCNTs ≈ 5B-oCNTs < 5P-oCNTs (Supporting Information, Figure S1). The onset temperature and peak position shift to higher temperature with an increasing amount of boron oxide. The modification with borate and phosphate is indeed reported to block the combustion sites serving as a point of attack for gaseous oxygen, and thus to suppress the combustion of the carbon framework at elevated temperatures.[12,13] From a kinetic point of view, this protective effect of boron oxide modification against O_2 activation is reflected by an approximately 40 kJ mol^{-1} higher activation energy of O_2 conversion (Figure 1a). However, the activation of propane is not affected; the activation energy remains at (130 ± 5) kJ mol^{-1}.

The modified CNTs are much more selective than a variety of supported vanadia catalysts (Supporting Information, Figure S2).[14] For propene selectivity at 673 K, the following trend could be observed: VO_x-Al_2O_3 > 2B/5B-oCNTs ≈ VO_x-TiO_2 > 5P-oCNTs > VO_x-CeO_2 > VO_x-SiO_2 > VO_x-ZrO_2 > (o)CNTs. The decreasing selectivity with ongoing conversion is due to the weaker C–H bonds in propene and its resulting combustion.[9] Total oxidation of propane is suppressed by boron and phosphorus modification, as seen by an almost 100% propene selectivity by extrapolating to zero propane conversion. Only an sp^2-hybridized carbon atom allows stable and selective ODH catalysis.[15] For this study, CNTs were chosen as they are a compromise between high reactivity (sp^3, activated carbon) and high stability (sp^2, graphite). The compromise is motivated by the poor performance in ODH provided by a reference sample of activated carbon loaded with 5 wt% B_2O_3 (Supporting Information, Figure S3).

Microscopic, spectroscopic, and thermoanalytic techniques were employed to investigate the structural and surface properties of catalysts before and after reaction. Energy-filtered transmission electron microscopy (EF-TEM) shows that both boron and oxygen are highly dispersed throughout the CNT substrate (Supporting Information, Figure S4). The composite is stable under reaction conditions, and all of the B_2O_3 (1.7 atom% B for 5B-oCNT) could be detected by electron energy-loss spectroscopy (EELS) after use in ODH (Supporting Information, Figure S5). The CNT framework was not affected by modification by heteroatoms or the oxidative reaction atmosphere, as shown by subsequent characterizations by Raman spectroscopy, scanning and transmission electron microscopy (SEM and TEM), and N_2 physisorption (Supporting Information, Figures S1 and S5). As an indication of the disorder of carbon atoms, the ratio of the *D* band to the *G* band decreases slightly, and it varies between 2.0 and 2.1 (Supporting Information, Table S1). The SEM and TEM images show that fresh and used samples have a similar morphology. The position of the major peak in the TPO curves is almost the same; however, a low-temperature peak at around 550 K disappears, which is probably due to the removal of some combustible functionalities in the oxidative reactant flow. The qualitative and quantitative change in oxygen surface functionalities was monitored by temperature-programmed desorption (TPD) and thermogravimetric analysis (TGA; Supporting Information, Figure S6).

The initial evolution of catalytic performance of pristine and modified CNT samples is illustrated in the Supporting Information, Figure S7. During the time on-stream, pristine and oxidized CNTs increase in activity. This result can be explained by the in-situ generation of active groups and/or elimination of labile functional groups and amorphous carbon debris in the oxidizing feed-gas atmosphere,[16] which is in agreement with TPO and TPD results. A lower degree of disorder accompanied by a loss of near-surface oxygen is observed by Raman spectroscopy and also by ex-situ X-ray photoelectron spectroscopy (XPS) and TPD, respectively (Supporting Information, Table S1). In general, the TPD analysis of fresh and used CNT samples shows a loss of labile carboxy, anhydride, and lactone groups that release CO_2 between 400 and 800 K, and the formation of ketonic and quinoidic functionalities that release CO in the range 800–1200 K (Supporting Information, Figure S6).[2] The latter species dominate the active surface together with high-temperature-stable lactone and anhydride groups. The oCNT samples have a higher initial activity than pristine CNTs. However, after five hours, the difference in structure or catalysis becomes negligible. The activation period can be simulated by further oxidation of oCNTs (1 h, 773 K, air). A superior stable performance of the oCNTs is observed from the start of the reaction. Regarding the N_2 physisorption results, a general rise in surface area, and in particular within

the < 5 nm sized pores, may indicate a strong impact of the opening of closed carbon nanotubes at their ends by gas-phase oxygen during the ODH reaction. However, the active sites that are generated are unselective and favor CO_2 formation, as shown by a drastic decrease in propene selectivity within the initial period (Supporting Information, Figure S7).

In contrast, B_2O_3-modified CNTs deactivate to a small extent initially, which may be due to the decomposition or thermal spreading of the deposited B_2O_3 precursor. The balance between activity loss and selectivity gain can be tuned by controlling the amount of boron dopant (Figure 1b). Both overall activity and propene selectivity show a strong dependence on the boron oxide loading. Apart from the suppressed total combustion reaction on the modified CNTs, a further reason for enhanced propene selectivity may also be the lower reoxidation capacity of active sites. Boron oxide as an electron-deficient promoter tends to inhibit the dissociative adsorption of O_2 and thus sustains the selective oxygen species on the catalyst surface.[17] The effect of boron oxide was observed for a loading as low as 0.003 wt% (Figure 1b), thus clearly demonstrating that only a negligible fraction of surface functionalities detected by the applied characterization techniques are catalytically active. The propene selectivity increases from 17% to 28% whereas the overall reaction rate decreases from 4.3 to 3.2 mmol $g^{-1} h^{-1}$, resulting in an improved production of propene of up to 18%. The maximum productivity of propene was found at a B_2O_3 loading of 0.01 wt%. It should be noted that propene yield at the same conversion increases with the reaction temperature, whereas the thermal stability of B_2O_3-modified CNTs increases with increased loading. Thus the combined optimization of reaction conditions and boron oxide loading with regard to the propene yield is quite complex.

The oxygen exchange capabilities of oCNT samples with and without B_2O_3 modification were investigated by switching diluted $^{16}O_2$ with its $^{18}O_2$ isotope tracer. As shown in Figure 2a, oCNTs are very active in oxygen exchange, and a pronounced generation of $^{18}O^{16}O$ was observed even in the absence of propane. In contrast, the amount of $^{18}O^{16}O$ decreases with increasing B_2O_3 loading, and almost vanishes on the highly B_2O_3-loaded samples (Figure 2b). This phenomenon is similar to the case of a low-loaded VO_x-Al_2O_3 catalyst, which was studied herein as a reference system having a good ODH performance with propane.[14] Electrophilic intermediate oxygen species, such as peroxide or superoxide, on unmodified CNTs are most likely the cause of the high activity but low selectivity with propene.

The uniform nature of the active sites can be derived from the reaction and characterization measurements. Pristine and oxidized CNTs have a similar activity and selectivity in the steady state, and also similar apparent activation energies of propane conversion, oxygen conversion, and propene formation (Figure 1a). The same holds for the boron and phosphorus oxide modified nanotubes with 5 wt% loading. These results suggest that the surface domains activating the ODH turnover do not contain either boron or phosphorus, and these heteroatoms do not affect the nature of active sites. All the experiments show that the effect of boron and phosphorus

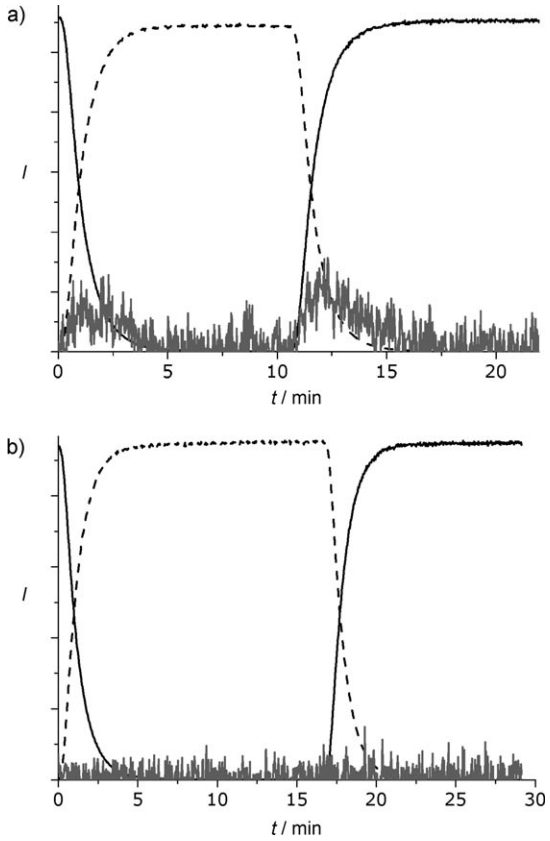

Figure 2. Oxygen exchange on a) oCNTs, and b) 5B-oCNTs, after the gas atmosphere was switched from 2% $^{16}O_2$/Ne to 2% $^{18}O_2$/2% Ar/96% Ne, 673 K, 100 mg, 10 $mL_n\,min^{-1}$ given as ion current *I*. Black sold line: $^{16}O_2$, black dashed line: $^{18}O_2$, gray solid line: $^{16}O^{18}O$ (magnified 300 times).

oxide is to block or cover the combustion sites on the surface or the groups causing CO_x formation, and is in agreement with the TEM/EELS and XPS results (Supporting Information, Figures S5 and S8). Owing to the chosen preparation method, the majority of amorphous B_2O_3 is deposited in the cavity and on the tips of CNTs.[18] Only a minor fraction of the outer CNT surface is covered by an amorphous coating of about 1–2 nm thickness, whereas a highly dispersed submonolayer deposition of BO_x species is expected to be omnipresent, as the reduced surface area of modified CNTs may also be interpreted as the filling of surface defects and holes in the graphene layers. The good thermal stability of the doped samples during TPO indicates a covalent bonding to the CNT structure, whereas the B_2O_3/P_2O_5 filling of the CNTs acts as a backbone against oxidation.

An insight into the origin of high activities and selectivities of vanadia and modified CNTs compared to unmodified CNTs is obtained by an experiment with periodic feeds of propane and oxygen. Figure 3a–c shows the transient responses of reaction products as propane flows over the oxygen-treated surface. A large amount of CO and CO_2 is quickly formed over unmodified CNTs, showing that the direct combustion pathway of propane occurs to some degree. However, the interaction of propane with oxygen-treated surfaces of the modified CNTs and VO_x-Al_2O_3 preferentially yields propene, whereas the total combustion to CO_x occurs

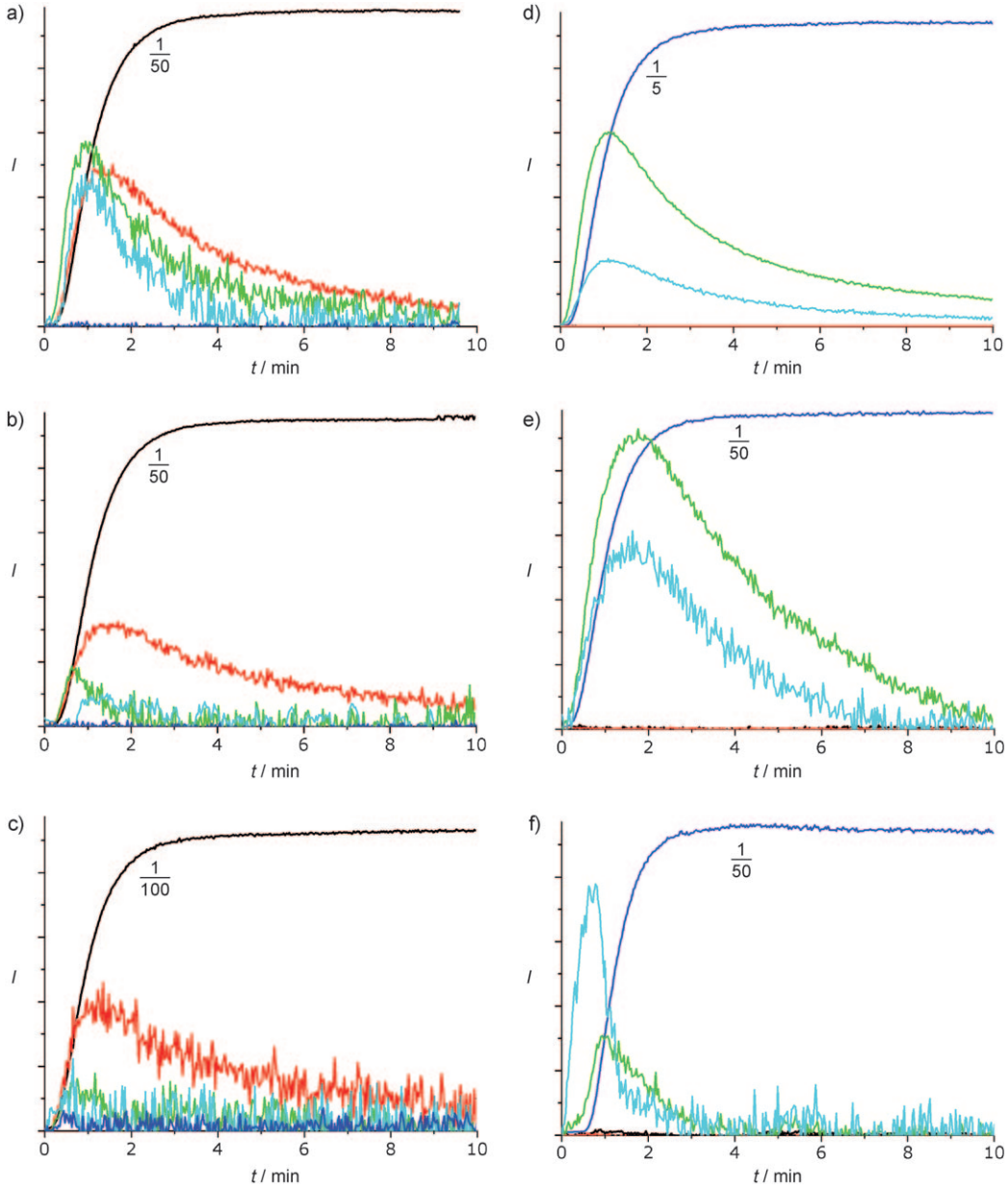

Figure 3. Periodic feed experiments. Step marking of 2% C_3H_8/He on freshly oxidized catalyst (a–c) and of 2% O_2/He on propane-reduced catalyst (d–f). a,d) oCNTs, b,e) 5B-oCNTs, c,f) VO_x-Al_2O_3; 673 K, 100 mg, 10 $mL_n\,min^{-1}$. Black C_3H_8, red C_3H_6, green CO_2, cyan CO, blue O_2. The numbers on the curves indicate the decrease relative to the other curves.

only to a small degree. It is clear that each carbon catalyst yields a similar amount of propene, especially taking into account the different surface area and amount of surface oxygen (Supporting Information, Table S1, Figure S8). This result indicates that surface modification with B_2O_3 solely affects non-selective active sites, as it has been shown for P_2O_5 in the ODH of *n*-butane.[4] With regard to the overall activity, the amount of reaction products formed on the vanadia catalyst is very low. From these results, we can therefore estimate the specific turnover frequency on carbon-based active sites to be approximately 30 times lower than that on vanadia sites in VO_x-Al_2O_3.[14]

One reason for this effect can be derived from subsequent reoxidation of the catalysts reduced by the reaction with propane (Figure 3d–f). The amount of propane adsorbed on the vanadia catalyst is very small and its elimination by combustion is very fast compared to CNT catalysts. For carbon catalysts, there is a much higher amount of propane adsorbed on the surface, sticking on the active sites to result in a huge amount of CO_x before reoxidation of the active site. Consequently, CNT catalysts have a superior performance under oxygen-rich reaction conditions (Supporting Information, Figure S9). Vanadia catalysts, the most selective metal-based catalysts, can work well at a low partial pressure of oxygen owing to suppression of consecutive propene combustion. The critical issue of self-oxidation stability has been accounted for by long-term studies of selected catalysts (Supporting Information, Figure S10). Using an oxygen-to-hydrocarbon ratio of 1:1, VO_x-Al_2O_3, 5B-oCNTs, and even non-modified oCNTs provide stable catalytic performance

for a time-on-stream of up to 200 h. Using diluted feeds, 5B-oCNTs at similar conversion give a similar propene selectivity to VO_x-Al_2O_3.[12] A steady increase in activity of 5B-oCNTs whilst maintaining the high selectivity shows the potential in synthesizing more optimized catalysts in the near future.

Nanocarbons are an attractive alternative to metal oxide catalysts for ODH reactions of not only ethylbenzene but also light alkanes. Propane molecules are activated by the surface oxygen groups to yield propene with a remarkable selectivity. Propane adsorption on the reduced catalyst surface, which appears to be detrimental for alkene selectivity, can be efficiently reduced by modification with a small amount of boron oxide. This, on the other hand, will suppress formation of non-selective oxygen species. One of the remaining drawbacks is the low overall activity of carbon catalysts, which can be overcome by fabricating a high concentration of selective sites on the surface.

Experimental Section

Catalyst preparation and characterization: Pristine carbon nanotubes (CNTs) were obtained from Nanocyl (NC 3100). CNTs were refluxed in concentrated nitric acid (100 $mL\,g_{CNT}^{-1}$) for 2 h, washed with deionized water to pH 6–7, and dried in air at 393 K overnight (oCNTs). B- and P-modified samples were prepared by incipient wetness impregnation of oCNTs (6 $mL\,g^{-1}$) using aqueous solutions of $(NH_4)_2B_{10}O_{16}{\cdot}8H_2O$ and $(NH_4)_2HPO_4$ (Sigma Aldrich, >99%), to achieve loadings of between $x = 0.003$ and 5 wt% B_2O_3 or 5 wt% P_2O_5. Impregnated samples were dried in air at 393 K overnight (xB-oCNTs, 5P-oCNTs). Specific surface areas (BET) and pore size distributions (BJH) of the CNT samples were determined by N_2 physisorption at 77 K using a Micromeritics 2375 BET apparatus. Relative amounts of disordered (D) and graphitic (G) carbon species were determined by laser Raman spectroscopy using an ISA LabRam instrument equipped with an Olympus BX40 microscope attachment. Excitation wavelength was 632.8 nm and a spectral resolution of 0.9 cm^{-1} was used. TEM was performed using a Philips CM200 FEG transmission electron microscope (accelerating voltage 200 kV) using high-resolution imaging, EELS, and EDX (energy-dispersive X-ray spectroscopy). Elemental mapping was conducted under STEM mode with the EDX detector as recorder. SEM images were obtained with a HITACHI S-4800 instrument (cold FEG in SE and in quasi BSE mode with accelerating voltage of 2–15 kV). Elemental analysis was performed using an EDAX Genesis 4000 System equipped with a sapphire detector. Information about the carbon species with different resistance against oxidation was obtained by TPO. 20 mg of sample was heated linearly in a quartz tubular reactor from 323 to 1100 K in a 15 $mL_n\,min^{-1}$ flow of 13.3 vol% O_2 in He. The product gas was analyzed by on-line MS (Pfeiffer QME 200); the masses 4, 17, 18, 28, 32, and 44 were monitored for the detection of He, NH_3, H_2O, CO, O_2, and CO_2 with a time-resolution of 4 s. Surface analyses by XPS were performed at ISISS beam line at BESSY II, Berlin, Germany. The XP spectra were corrected for beam intensity. Prior to fitting, a Shirley background was subtracted. Peak areas were normalized with theoretical cross-sections to obtain the relative surface compositions.

Catalytic testing: A standard catalytic testing procedure was performed in a set-up described elsewhere.[14] Respectively 1 g of granulated CNT sample (100–450 μm) was kept at 673 K in a 60 $mL_n\,min^{-1}$ flow with $C_3H_8/O_2/N_2 = 1{:}1{:}4$ until constant conversion was achieved. Thereafter, the total flow rate was varied between 10–120 $mL_n\,min^{-1}$. The apparent activation energy was determined by step-wise cooling (10 K steps) down to 623 K at 60 $mL_n\,min^{-1}$. For steady-state isotope transient kinetic analysis (SSITKA) and periodic feed experiments, 100 mg of sample were used with a flow rate of 10 $mL_n\,min^{-1}$ and aging period of 5 h in a $C_3H_8/O_2/N_2 = 1{:}1{:}4$ stream. The following gas mixtures were used: 2% $^{16}O_2$/He, 2% C_3H_8/He, 2% $^{16}O_2$/98% Ne, and 2% $^{18}O_2$/2% Ar/96% Ne.

Received: April 5, 2009
Revised: July 2, 2009
Published online: August 7, 2009

Keywords: C–H activation · heterogeneous catalysis · nanomaterials · oxidation · selectivity

[1] H. P. Boehm, *Carbon* **1994**, *32*, 759.
[2] J. L. Figueiredo, M. F. R. Pereira, M. M. A. Freitas, J. J. M. Órfão, *Carbon* **1999**, *37*, 1379, and references therein.
[3] a) K. P. de Jong, J. W. Geus, *Catal. Rev. Sci. Eng.* **2000**, *42*, 481; b) P. Serp, M. Corrias, P. Kalck, *Appl. Catal. A* **2003**, *253*, 337; c) A. Rochefort, P. Avouris, *J. Phys. Chem. A* **2000**, *104*, 9807; d) Y. Maniwa, Y. Kumazawa, Y. Saito, H. Tou, H. Kataura, H. Ishii, S. Suzuki, Y. Achiba, A. Fujiwara, H. Suematsu, *Mol. Cryst. Liq. Cryst.* **2000**, *340*, 671; e) J. L. Figueiredo, M. F. R. Pereira, *Catal. Today* **2009**, DOI: 10.1016/j.cattod.2009.04.010.
[4] J. Zhang, X. Liu, R. Blume, A. Zhang, R. Schlögl, D. S. Su, *Science* **2008**, *322*, 73.
[5] J. A. Maciá-Agulló, D. Cazorla-Amorós, A. Linares-Solano, U. Wild, D. S. Su, R. Schlögl, *Catal. Today* **2005**, *102–103*, 248.
[6] a) D. S. Su, N. Maksimova, J. J. Delgado, N. Keller, G. Mestl, M. J. Ledoux, R. Schlögl, *Catal. Today* **2005**, *102–103*, 110; b) X. Liu, D. S. Su, R. Schlögl, *Carbon* **2008**, *46*, 547; c) M. F. R. Pereira, J. L. Figueiredo, J. J. M. Órfão, P. Serp, P. Kalck, Y. Kihn, *Carbon* **2004**, *42*, 2807; d) D. E. Resasco, *Nat. Nanotechnol.* **2008**, *3*, 708; e) J. Sui, J. H. Zhou, Y. C. Dai, W. K. Yuan, *Catal. Today* **2005**, *106*, 90.
[7] a) K. Chen, A. Khodakov, J. Yang, A. T. Bell, E. Iglesia, *J. Catal.* **1999**, *186*, 325; b) P. Mars, D. W. van Krevelen, *Chem. Eng. Sci.* **1954**, *3*, 41.
[8] a) G. Mul, M. A. Bañares, G. Garcia Cortéz, B. van der Linden, S. J. Khatib, J. A. Moulijna, *Phys. Chem. Chem. Phys.* **2003**, *5*, 4378; b) A. T. Bell in *Catalyst Deactivation* (Eds.: E. E. Petersen, A. T. Bell), Marcel Dekker, New York, **1987**, pp. 235–260.
[9] B. K. Hodnett in *Supported Catalysts and Their Applications* (Eds.: D. C. Sherrington, A. P. Kybett), Royal Society of Chemistry, London, **2000**, pp. 1–8.
[10] a) E. A. Mamedov, V. Cortés Corberán, *Appl. Catal. A* **1995**, *127*, 1; b) I. E. Wachs, *Catal. Today* **2005**, *100*, 79; c) F. Cavani, N. Ballarini, A. Cericola, *Catal. Today* **2007**, *127*, 113.
[11] a) H. W. Zanthoff, S. A. Buchholz, A. Pantazidis, C. Mirodatos, *Chem. Eng. Sci.* **1999**, *54*, 4397; b) B. Grzybowska-Świerkosz, *Appl. Catal. A* **1997**, *157*, 409.
[12] L. E. Jones, P. A. Thrower, *J. Chim. Phys.* **1987**, *84*, 1431.
[13] a) D. W. McKee, *Chem. Phys. Carbon* **1991**, *23*, 173; b) Y. J. Lee, L. R. Radovic, *Carbon* **2003**, *41*, 1987.
[14] a) B. Frank, A. Dinse, O. Ovsitser, E. V. Kondratenko, R. Schomäcker, *Appl. Catal. A* **2007**, *323*, 66; b) A. Dinse, B. Frank, C. Hess, D. Habel, R. Schomäcker, *J. Mol. Catal. A* **2008**, *289*, 28.
[15] a) D. S. Su, N. Maksimova, J. J. Delgado, N. Keller, G. Mestl, M. J. Ledoux, R. Schlögl, *Catal. Today* **2005**, *102–103*, 110; b) J. Zhang, D. S. Su, A. H. Zhang, D. Wang, R. Schlögl, C. Hébert, *Angew. Chem.* **2007**, *119*, 7460; *Angew. Chem. Int. Ed.* **2007**, *46*, 7319.
[16] K. Behler, S. Osswald, H. Ye, S. Dimovski, Y. Gogotsi, *J. Nanopart. Res.* **2006**, *8*, 615.
[17] a) E. V. Kondratenko, M. Cherian, M. Baerns, *Catal. Today* **2006**, *112*, 60; b) O. V. Buyevskaya, M. Baerns, *Catal. Today* **1998**, *42*, 315.
[18] J. Zhang, Y. S. Hu, J. P. Tessonnier, G. Weinberg, J. Maier, R. Schlögl, D. S. Su, *Adv. Mater.* **2008**, *20*, 1450.

